# Diffusion and dynamical transition in hierarchical systems

S. Teitel
*Department of Physics and Astronomy, University of Rochester, Rochester, New York 14627*

D. Kutasov and E. Domany
*Department of Electronics, The Weizmann Institute of Science, 76 100 Rehovot, Israel*
(Received 14 October 1986)

We have recently found a phase transition in the dynamics of a particle that diffuses in the presence of a hierarchical array of barriers. The transition occurs as $R$, a parameter that controls the relative size of the barriers, is varied. For $R > R_c$, the system is diffusive; as $R \to R_c^+$ the diffusion constant vanishes. For $R < R_c$, the system is subdiffusive; the mean-square displacement grows slower than linearly with time, with an exponent that varies continuously with $R$. Analytic as well as numerical renormalization-group methods are introduced and used to solve some specific models; however, the tools developed here are applicable to more general situations as well. In one dimension we present, in addition to a renormalization-group solution for the asymptotic behavior, several new results; in particular, scaling arguments that predict *transient* behavior as well. We show that the asymptotic regime is approached algebraically, on time scales that obey a law of a Vogel-Fulcher form near the transition. Higher-dimensional systems that also have such a transition are introduced and studied. Finally, possible connections to many-body systems such as dynamic spin models and glassy materials are suggested and discussed.

## I. INTRODUCTION

Judging on the basis of recent literature, anomalous relaxation appears to be the rule rather than the exception in many dynamic processes. Relaxation to equilibrium in glassy materials[1] often follows a stretched exponential law.[2] Electron-hole transport in amorphous semiconductors is governed by algebraic relaxation (recombination).[3,4] Anomalous relaxation processes were observed in a variety of systems and models, that include spin glasses,[5] diffusion limited chemical reactions[6] and photoexcited proteins.[7] Some of the systems of interest are of high technological relevance, such as particulate materials used for magnetic recording,[8] that exhibit anomalous decay of the magnetization. Others are of less applied, but high theoretical interest, such as fractals, for which diffusion is anomalous.[9]

A number of recent theoretical papers considered a variety of models that exhibit anomalous dynamics. Palmer *et al.*[1] consider hierarchically constrained glassy dynamics, in which slow degrees of freedom can relax only after the faster processes have taken place. Klafter and Shlesinger[10] have shown, that this model yields results similar to what can be obtained by two other theories. Diffusion in ultrametric spaces was considered by a number of groups, and shown to yield anomalous behavior, the nature of which depends on assumptions made on the hopping rates.[11] The spaces considered[11] can be viewed as the lowest levels (leaves) of various trees, with hopping between any two leaves possible, with rates that depend on their (ultrametric) distance.

A central common feature of all systems and models mentioned is the existence of a *hierarchy of time scales* associated with various stages of the relaxation process. A particularly simply model, in which this basic feature appears in a straightforward manner, was recently studied by Huberman and Kerszberg[12] (HK). They considered diffusion on a linear chain, with a hierarchically assigned set of barriers between neighboring sites (See Fig. 1). Denoting by $R$ a parameter that controls the relative strength of barriers, HK were able to analyze the problem in the $R \ll 1$ limit (which corresponds, for the case of thermal activation, to $T \to 0$). HK found[12] the surprising result that the autocorrelation function decays algebraically, e.g., $P_0(t) \sim t^{-x(R)}$, with a power $x(R)$ that varies continuously with $R$. The intriguing question, how this behavior is connected to the normal diffusion result $x = \frac{1}{2}$, expected at $R = 1$, was resolved[13] by identifying a dynam-

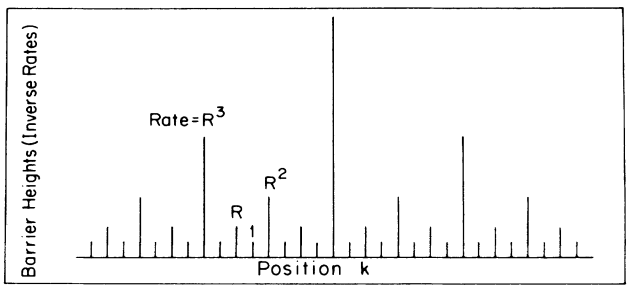


FIG. 1. Hierarchical barrier structure. The height of a barrier is inversely proportional to the transition rate. The largest rate (smallest barrier) is normalized to 1. The other rates are given by $R^l$ ($0 \le R \le 1$, $l$ is an integer) where $l$ denotes the level of the hierarchy, as illustrated.

 

ic transition at $R_c$:

$$P_0(t) \sim \begin{cases} [D(R)t]^{-1/2}, & R > R_c \\ t^{-x(R)}, & R < R_c . \end{cases} \tag{1.1}$$

Such a transition was first observed by Alexander *et al.*[14] These authors considered diffusion in one-dimensional random systems, with nearest-neighbor hopping rates $W$, taken from a distribution $P(W)$. In particular, they studied the long time behavior of the autocorrelation function and its dependence on the behavior of $P(W)$ for $W \to 0^+$.

It should be emphasized that one dimensional *diffusion* problems of the kind discussed have trivial steady state solutions.[15] The inverse diffusion constant $D^{-1}$ is given by the average inverse transition rates.[14] This relationship holds[16] as long as $D > 0$.

In this paper we present details of a previously reported investigation[13] (Secs. II and III) as well as several extensions and new results (Sec. IV and on). In Sec. II we introduce a renormalization-group (RG) –based framework to solve such problems. Our solution applies in the *nontrivial,* subdiffusive regime as well. The renormalization group ideas are implemented in Sec. III, in three different ways; decimation,[17] perturbation theory and numerical evaluation of the $\beta$ function.[13,18] The pertubative approach allows us to solve the problem in more than one dimension. The numerical approach we present can also be used for higher dimensional and more general diffusion problems. Thus we are able to go way beyond the trivial evaluation of the diffusion constant. It should be noted that as opposed to the models of Ref. 11, in the classes treated here the topology of the space is regular, not ultrametric; only the hopping rates between neighboring sites are assigned hierarchically.

In Sec. IV we compute various physically relevant quantities. First we show how the diffusion constant can be derived from the RG formalism. Next we derive the diffusion constant for $R > R_c$ using the standard argument.[14–16] Subsequently a simple, scaling derivation of the result (1.1) in the *subdiffusive regime* is presented. Two other issues of interest are addressed in Sec. IV. We consider the problem of transient (nonasymptotic) behavior. It is shown that the dynamic process satisfies a generalized diffusion equation: $\langle X^2(t) \rangle = 2D(X(t))t$ where $D(X)$ is a local diffusion constant determined by the barriers which have, on the average, been passed over at time $t$. $\langle X^2(t) \rangle$ as well as $D(X)$ are calculated analytically and by numerical simulation. The two methods are in excellent agreement. Using the analytic form of $D(X)$, we estimate the time it takes for the system to approach the asymptotic regime. Surprisingly, a Vogel-Fulcher–type law[19] is found. Subsequently, motion in a constant force field superimposed on the hierarchical barriers is studied analytically[20] and numerically. For small force the Einstein relation between mobility and the diffusion constant is found.

In Sec. V, a problem of hierarchical barriers in $d > 1$ dimensions is solved using the perturbative approach of Sec. III. Our results are discussed and summarized in Sec. VI.

## II. MODEL AND RENORMALIZATION-GROUP METHOD

### A. Statement of model

The model we consider,[12] shown in Fig. 1, consists of a linear chain of sites $k = 1, 2, \ldots, N = 2^n$. A particle can hop from site $k$ to sites $k \pm 1$ with transition rates $W_{k,k\pm1} = W_{k\pm1,k}$. The motion is governed by a master equation for the probability $P_k(t)$ for the particle to be at site $k$ at time $t$. Probability conservation gives

$$\frac{dP_k}{dt} = W_{k,k+1}(P_{k+1} - P_k) + W_{k-1,k}(P_{k-1} - P_k) \equiv -\sum_{k'} M_{k,k'} P_{k'} , \tag{2.1}$$

where the rates $W_{k,k+1}$ define the master equation matrix $M_{k,k'}$. The rates $W_{k,k+1}$ of our model are assigned hierarchically as shown in Fig. 1 (the transition rate is the inverse of the barrier height).

$$W_{k,k+1} = R^m, \quad R < 1$$

if $k(\mathrm{mod}2^l) = 0$ for all $l \le m$. At the boundaries we take confining walls, i.e., $W = 0$.

From (2.1), it is clear that the time evolution of the system will be controlled by the eigenvalues $\{\lambda_i\}$ of the master equation matrix $M_{k,k'}$. To make this connection precise, it is convenient to consider the autocorrelation function $P_0(t)$, defined as the probability that the particle is at time $t$ at the same position it started from at time $t = 0$, averaged over all starting positions. In Appendix $A$ we rederive the relationship

$$P_0(t) = \int_0^\infty g(\lambda) e^{-\lambda t} d\lambda , \tag{2.2}$$

where $g(\lambda) = N^{-1} \sum_i \delta(\lambda - \lambda_i)$ is the density of eigenvalues of $M_{k,k'}$. We will be interested only in the long time asymptotic behavior of the system as the size $N \to \infty$. From Eq. (2.2) we clearly see that the long time behavior is governed by the low-lying eigenvalues of $M$, i.e., $g(\lambda)$ as $\lambda \to 0$.

A second convenient measure of the asymptotic time evolution of the system is the average distance squared traveled by the particle in a time $t$, $\langle X^2(t) \rangle$. A scaling argument, which we rederive in Appendix A, relates this quantity to the autocorrelation function

$$\langle X^2(t) \rangle \sim P_0(t)^{-2} \quad \text{as } t \to \infty . \tag{2.3}$$

Sections II B and III are devoted to the calculation of $P_0(t)$ as $t \to \infty$, via the calculation of the density of states $g(\lambda)$ as $\lambda \to 0$.

### B. Renormalization-group method: General formalism

The method we use to calculate the density of states $g(\lambda)$ is the renormalization group. Such an approach is suggested by the self-similar structure of the hopping rates. We will discuss three different implementations of the RG as applied to this problem: decimation, perturbative, and numerical, which together allow us to predict the behavior of our model for the complete range of the

parameter $0 \leq R \leq 1$.

Although the implementation in each case will be slightly different, the RG framework used will be the same. Hence we discuss the general framework first. The main idea is to regard $R$, the parameter of our model (the ratio of transition rates from one level of the hierarchy to the next), as the scaling parameter of a RG transformation. We compare a system of size $2^n$ described by the matrix $M_{kk'}(R)$ at parameter $R$, to a system of size $2^{n-1}$ described by the matrix $M'_{kk'}(R')$ at a new value of the parameter $R'$. We wish to choose this new $R'$ such that the long time behavior of the two systems will be the same in the limit $n \to \infty$. This procedure determines a recursion relation

$$R' = \beta(R) ,$$

which describes how the system scales after the smallest barriers have been eliminated from the problem. The recursion relation determines the flows and fixed points of our RG transformation. It is supplemented by a relation that describes how the density of states $g(\lambda)$ of the original problem is related to that of the new problem. Solution of this scaling relation for $g(\lambda)$ at the fixed points, $R^* = \beta(R^*)$, allows one to solve for $g(\lambda)$ at general $R$, as explained in detail below.

The condition that the two systems, described by $M(R,2^n)$ and $M'(R',2^{n-1})$, have the same long time behavior can be restated precisely in terms of the eigenvalues of these matrices, $\{\lambda_i\}$ and $\{\lambda'_i\}$. We require

$$\lambda'_i(R') = \alpha(R)\lambda_i(R) \quad \text{as } \lambda_i \to 0, \quad n \to \infty \tag{2.4}$$

i.e., the low-lying eigenvalues of the two systems should be related by a simple scale factor $\alpha(R)$. Such a condition ensures that as $n \to \infty$, the autocorrelation functions $P_0(t)$ will have the same asymptotic long time behavior, within a rescaling of time (see also Sec. IV A).

We stress at this point, that there is no *a priori* way to know that an $R' = \beta(R)$ can in fact be found such that scaling, as in Eq. (2.4), exists. This is merely the statement of our scaling *hypothesis,* which must be explicitly verified by the specific implementation of the RG, which will also enable us to calculate the functions $\alpha(R)$ and $\beta(R)$. We further stress that we look for such matching only in the long time limit, i.e., as $\lambda \to 0$.

Assuming such scaling exists, we now derive a recursion relation for the density of states under the RG transformation, in terms of the functions $\alpha(R)$ and $\beta(R)$. Using the definition of $g(\lambda)$ in terms of the $\lambda_i$'s, equation (2.4) and $N' = N/2$ we have

$$g(\lambda) \equiv \frac{1}{N}\sum_i \delta(\lambda - \lambda_i) = \frac{1}{2N'}\sum_i \delta\left[\lambda - \frac{\lambda'_i}{\alpha}\right] = \frac{\alpha}{2}\frac{1}{N'}\sum_i \delta(\alpha\lambda - \lambda'_i) = \frac{\alpha}{2} g'(\alpha\lambda) .$$

Therefore the recursion relation for the density of states is

$$g(\lambda, R) = \frac{\alpha(R)}{2} g(\alpha(R)\lambda, \beta(R)) . \tag{2.5}$$

The above recursion relation is valid for all $R$, but we are particularly interested in solving it at the fixed points $R^* = \beta(R^*)$. At such $R^*$ we have

$$g(\lambda) = \frac{\alpha^*}{2} g(\alpha^*\lambda) , \tag{2.6}$$

where $\alpha^* = \alpha(R^*)$. The solution is found by assuming a power-law form for $g(\lambda)$ and thus finding

$$g(\lambda) \sim \lambda^{-y}, \quad y = 1 - \ln 2/\ln\alpha^* . \tag{2.7}$$

Substituting this into Eq. (2.2) we get for the autocorrelation function at the fixed point $R^*$,

$$P_0(t, R^*) \sim t^{-x} , \quad x = 1 - y = \ln 2/\ln\alpha^* . \tag{2.8}$$

If our RG procedure is self-consistent, i.e., scaling as in (2.4) holds, we expect that for any initial value of $R$ the system will flow, under the RG transformation, to some final fixed point $R^*(R)$. The long time behavior of the autocorrelation function at $R$ will thus be algebraic, with an exponent given by (2.8) determined by the behavior at the attracting fixed point $R^*(R)$.

## III. RENORMALIZATION-GROUP IMPLEMENTATIONS

What needs to be done is to calculate the flows from $\beta(R)$, and the scale factor $\alpha(R)$ at the fixed points $R^*$. There are various ways of accomplishing this. We first discuss the method of decimation.

### A. Decimation method

This method[17] consists of taking the set of equations (2.1) and explicitly solving for the probability $P_i$ at every other site [those marked by an $x$ in Fig. 2(a)] in terms of the probability at its neighbors $P_{i+1}$ and $P_{i-1}$. This is possible since the master equation (2.1) only connects nearest-neighbor sites. The resulting set of equations describe a system of half the size, and so if the new effective hopping rates between sites $i-1$ and $i+1$ have the same hierarchical structure as in the original problem, though perhaps with a new value of $R$, we can read off the desired scaling functions $\beta(R)$ and $\alpha(R)$.

It is more convenient to work here with the Laplace transform of the master equation (2.1) or equivalently the eigenvector equations of the matrix $M_{k,k'}$. If $\psi$ is an eigenvector of $M$ with eigenvalue $\lambda$, the explicit equations for three nearest-neighbor sites 1, 2, and 3 [see Fig. 2(a)] are

$$\begin{aligned} -\lambda\psi_2 &= W_{12}\psi_1 + W_{23}\psi_3 - (W_{12}+W_{23})\psi_2 , \\ -\lambda\psi_1 &= W_{01}\psi_0 + W_{12}\psi_2 - (W_{01}+W_{12})\psi_1 , \\ -\lambda\psi_3 &= W_{23}\psi_2 + W_{34}\psi_4 - (W_{23}+W_{34})\psi_3 . \end{aligned} \tag{3.1}$$

Solving for the decimated sites $\psi_1$ and $\psi_3$ and substituting into the equation for $\psi_2$ gives

$$-\lambda[1+a]\psi_2 = c_0\psi_0 + c_4\psi_4 - [c_0+c_4]\psi_2 , \tag{3.2a}$$

where

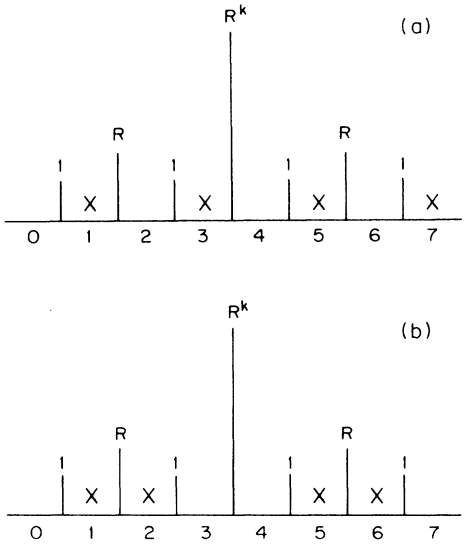


FIG. 2. Section of the hierarchical structure near a barrier of rate $R^k$. We decimate over sites marked by an $\times$ by solving for the probability at these sites in terms of their neighbors. Substituting the results back into the master equation eliminates these sites from the problems. In (a) decimation is over every other site (sites 1,3,5,7,. . . ) and corresponds to the analysis of Sec. III B. (b) Representation of the decimation scheme of Maritan and Stella (Ref. 22), where every other *pair* of sites is eliminated (sites 1,2,5,6,. . . ).

$$a=\frac{W_{12}}{W_{01}+W_{12}-\lambda}+\frac{W_{23}}{W_{23}+W_{34}-\lambda}\ ,$$
$$c_0=\frac{W_{01}W_{12}}{W_{01}+W_{12}-\lambda},\quad c_4=\frac{W_{23}W_{34}}{W_{23}+W_{34}-\lambda}\ . \tag{3.2b}$$

Since we are only interested in the $\lambda\to 0$ limit (asymptotically long times), we can set $\lambda=0$ in the terms $a,c_0,c_4$ to regain a master equation of the form (2.1). We wish to normalize the new effective hopping rates of Eq. (3.2) to have the same form as the original problem, i.e., the lowest barrier, now between sites 0 and 2, should have a rate of unity. We thus divide all terms in Eq. (3.2a) by $c_0$ and read off the new hopping rates and eigenvalues;

$$W'_{02}=1,\quad W'_{24}=c_4/c_0,\quad \lambda'=\lambda[1+a]/c_0\ . \tag{3.2c}$$

Finally we have to check that the new rates $W'_{24}$ have the same hierarchical structure as the original problem, and that $\lambda'$ is independent of position in the chain. For the choice of sites as in Fig. 2(a), i.e.,

$$W_{01}=W_{23}=1,\quad W_{12}=R,\quad W_{34}=R^k\ , \tag{3.2d}$$

we consider two limits, $R\ll 1$, and $R\simeq 1$.

### 1. The $R\ll 1$ limit

We find

$$W'_{24}=R^{k-1}[1+O(R)]\ , \tag{3.3a}$$
$$\lambda'=2\lambda[1+O(R)]/R\ . \tag{3.3b}$$

From (3.3a) we thus see that as $R\to 0$, the hierarchical structure is maintained with a new parameter $R'$ exactly equal to the old $R$, i.e., for $R\ll 1$, all $R$ are fixed points of this decimation. Thus we have the results, as $R\to 0$:

$$\beta(R)=R\ ,$$
$$\alpha(R)=(2/R)[1+O(R)]\ . \tag{3.4}$$

Substituting these results into Eq. (2.8) gives the autocorrelation function at small $R$

$$P_0(t)\sim t^{-x(R)},\quad x(R)=\frac{\ln 2}{\ln 2-\ln R}\ . \tag{3.5}$$

This is precisely the result of Huberman and Kerszberg[12] obtained by different methods.

### 2. The $R\approx 1$ limit

For $R=1-\delta$, $\delta\ll 1$, we find

$$W'_{24}=R^{(k-1)/2}[1+O(\delta)]\ , \tag{3.6a}$$
$$\lambda'=4\lambda[1+O(\delta)]\ . \tag{3.6b}$$

From (3.6a) we see that as $\delta\to 0$, the structure again remains hierarchical, but now with a new parameter $R'=\sqrt{R}$. Thus $R$ near 1 flows under successive iterations of the RG to the fixed point $R^*=1$. We have as $\delta\to 0$, i.e., $R\approx 1$,

$$\beta(R)=\sqrt{R}\ ,$$
$$\alpha(R)=4[1+O(\delta)]\ . \tag{3.7}$$

Using (3.7) in Eq. (2.8) gives, for the behavior at the $R^*=1$ fixed point,

$$P_0(t)\sim t^{-1/2} \tag{3.8}$$

the expected answer for the equal barrier chain, i.e., normal diffusion.

For a general value of $R$, the new effective rates $W'_{24}=c_4/c_0$ will not have the appropriate hierarchical structure; nonhierarchical couplings are generated. Thus the new decimated problem is not of the same form as the original one, and this RG scheme breaks down. However, the two limits where this scheme works, $R\ll 1$ and $R\simeq 1$, provide enough information to predict the qualitative structure at all $R$. At small $R$, there is a line of fixed points.[21] The autocorrelation function $P_0(t)$ has anomalously slow algebraic decay with an exponent that continuously varies as a function of $R$. (This is reminiscent of fixed line problems in usual thermodynamic RG's). For $R$ close to 1, the system flows into the $R^*=1$ fixed point which characterizes ordinary diffusion. There presumably exists therefore an intermediate critical value $R_c$ at which the line of fixed points present at small $R$ ends, and the flow to $R^*=1$ begins. Such an $R_c$ results in a sharp transition between the two regions of anomalous and ordinary diffusion. This scenario is now verified in the following sections.

We point out that an alternative decimation RG has recently been introduced in a very nice calculation by Maritan and Stella.[22] Instead of decimating over every other site as in Fig. 2(a), they choose to decimate over every

other *pair* of sites as in Fig. 2(b). The resulting decimated master equation is found to have the required hierarchical structure for all initial values of $R$. Exact recursion relations are found, which verify all our results that were previously found by the methods discussed below.[23]

### B. Perturbative RG

Although the decimation procedure discussed above strongly suggests a line of fixed points that terminates at a critical $R_c$, an alternative scenario is also possible; the $R \ll 1$ calculation could indicate that $R^*=0$ is marginally unstable, with no line of fixed points, and so no transition. To resolve this question, as well as to calculate $\alpha(R)$ to higher order in $R$, we need a new scheme which will allow a systematic expansion in powers of $R$. To do this, we calculate the eigenvalues of the master equation matrix $M_{k,k'}(R)$ directly, using ordinary Rayleigh-Schrödinger perturbation theory in $R$. Comparison of these eigenvalues for matrices of different sizes will enable us to extract the scaling functions $\alpha(R)$ and $\beta(R)$, as discussed in Sec. II B.

Rayleigh-Schrödinger perturbation theory is particularly easy in our case. To see this, note that the matrix (2.1) for a system of size $2^n$ can be easily decomposed as follows ($\underline{0}_{k\times k'}$ denotes a $k\times k'$ matrix of zeros):

$$\underline{M}(n)=\underline{M}_0(n)+\underline{M}_1(n)=\begin{bmatrix}\underline{M}(n-1) & \underline{0}_{2^{n-1}\times 2^{n-1}}\\ \underline{0}_{2^{n-1}\times 2^{n-1}} & \underline{M}(n-1)\end{bmatrix}+R^{n-1}\begin{bmatrix}\underline{0}_{(2^{n-1}-1)\times 2^{n-1}} & \\ 0\ 0\ \cdots\ 0\ 1\ -1\ 0\ 0\ \cdots\ 0 & \\ 0\ 0\ \cdots\ 0\ -1\ 1\ 0\ 0\ \cdots\ 0 & \\ \underline{0}_{(2^{n-1}-1)\times 2^{n-1}} & \end{bmatrix}. \tag{3.9}$$

The first term $\underline{M}_0$ represents the matrix for two decoupled half systems of size $2^{n-1}$. These half systems are coupled through the second matrix $\underline{M}_1$, the perturbation which describes hopping between the half systems over the largest barrier of rate $R^{n-1}$ connecting them [see Eq. (2.1)]. Because of the symmetry of the system, eigenvectors are always symmetric or antisymmetric with respect to reflection about this tallest middle barrier. So if $\psi(n-1)$ is an eigenvector of $\underline{M}(n-1)$, with eigenvalue $\lambda$, we construct as the zeroth-order eigenvectors of $\underline{M}(n)$, the symmetric and antisymmetric direct products of $\psi(n-1)$, i.e.,

$$\psi_{\pm}^{(0)}(n)=\frac{1}{\sqrt{2}}(\psi(n-1),\pm\psi(n-1)) . \tag{3.10}$$

If $\psi(n-1)$ is symmetric then it is clear that $M_1(n)\psi_+^{(0)}(n)=0$ and hence $\psi_+^{(0)}(n)$ remains an exact eigenvector of $\underline{M}(n)$ with eigenvalue $\lambda$. The remaining $\psi_-^{(0)}(n)$ gives rise to a new higher eigenvalue, separated from $\lambda$ by $O(R^{n-1})$. Similarly, if $\psi(n-1)$ is antisymmetric, then $\psi_-^{(0)}(n)$ is an exact eigenvector. Therefore, the eigenvalue spectrum changes as $n$ increases as schematically shown in Fig. 3. The splitting of each new eigenvalue from the old remaining one is given, to lowest order in $R$, by

$$\delta\lambda^{(1)}(n)=\langle\psi_-^{(0)}(n)\,|\,M_1(n)\,|\,\psi_-^{(0)}\rangle=2\left[\frac{R}{2}\right]^{n-1}, \tag{3.11}$$

where we use the fact the elements of $\psi_{\pm}^0(n)$ are, to lowest order in $R$, just $\pm 1/(2^n)^{1/2}$.

One can now calculate $\delta\lambda_i$ to higher order in $R$ by continuing the perturbation theory. Due to the recursive nature of the way $\underline{M}(n)$ is constructed from $\underline{M}(n-1)$, it can be seen that $\delta\lambda_i(n)$ has the following form:[24]

$$\delta\lambda_i(n)=2\left[\frac{R}{2}\right]^{n-1}[1+p_i(R)+O(R^{n-m_i})] . \tag{3.12}$$

The leading term is simply the first-order correction (3.11). $p_i(R)$ is an infinite series in $R$ (of lowest order $R$) which represents the higher-order corrections, in the limit $n\to\infty$. $p_i(R)$ is different for the different eigenvalues $i$, but does not depend on the system size $2^n$. The finite-size corrections to the $n\to\infty$ limit are of order $O(R^{n-m_i})$, where $m_i$ is some integer of order $\log_2 i$. The important point is that for $i$ finite, $m_i$ remains finite as $n\to\infty$.

Thus the ratio of splittings from level $n$ to $n-1$ is

$$\frac{\delta\lambda_i(n-1)}{\delta\lambda_i(n)}=\frac{2}{R}[1+O(R^{n-m_i-1})] . \tag{3.13}$$

For $n\to\infty$, but $i$ finite (i.e., $\lambda\to 0$) we thus see that $\lambda_i'(R,n-1)=(2/R)\lambda_i(R,n)$ or $\beta(R)=R$ and $\alpha(R)=2/R$. These are precisely the results of the decimation calculation, but now demonstrated to all order in $R$ as $n\to\infty$, $\lambda\to 0$. Thus our RG does have a fixed line, and the exponent for the autocorrelation function decay given in Eq. (3.5) is exact to all orders in $R$.

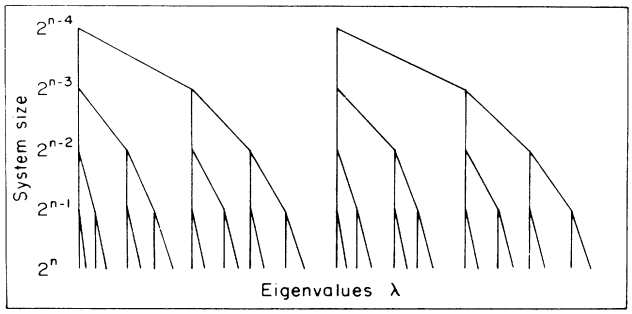


FIG. 3. Schematic representation of eigenvalues of the master-equation matrix (2.1) for systems of size $2^n$. All eigenvalues of a system of size $2^{n-1}$ remain eigenvalues of the system of size $2^n$. An additional eigenvalue splits off from each of these old ones by an amount of $O(R^{n-1}/2^{n-2})$.

### C. Numerical RG

In Sec. III B we have shown that to all orders in perturbation theory in $R$, we have $R'=\beta(R)=R$, i.e., a line of fixed points, and that $\alpha(R)=2/R$. However, from Sec. III A it is clear that this line of fixed points must terminate somewhere in the interval $0<R<1$. At some critical $R_c$ we expect level crossing to cause perturbation theory to break down, end the line of fixed points, and mark the transition to ordinary diffusion. To study this transition we now proceed to a numerical method. The RG procedure we follow[18] is analogous to that of the perturbation method of Sec. III B, only now we calculate directly (numerically), instead of perturbatively, the eigenvalues of the matrices $M(R,n)$. Although for our particular one dimensional problem we will find in Sec. IV a simpler way to directly compute this critical $R_c$, the method we outline in this section is completely general and should be applicable to other models and higher dimensions.

We compute low-lying eigenvalues for systems of sizes $2^9$ up to $2^{15}$. The matrices are tridiagonal and our algorithm, based on the negative eigenvalue theorem[25] combined with bisection, was found to be extremely efficient and stable. In Fig. 4 we plot the results for

$$\gamma=\lambda_1/\lambda_2 , \tag{3.14}$$

the ratio of two lowest nonzero eigenvalues, as a function of $R$. The limiting ($n\to\infty$) curve (dashed line) is clearly seen to be the straight line $\gamma(R)=R/2$ for $0\le R\le\frac{1}{2}$, which joins continuously the line $\gamma(R)=\frac{1}{4}$ for $\frac{1}{2}\le R\le 1$.

By comparing curves of $\gamma_n$ to $\gamma_{n-1}$ for finite $n$, we can construct the $\beta$ function $R'=\beta(R)$ by matching

$$\gamma_n(R)=\gamma_{n-1}(R') . \tag{3.15}$$

This ensures that these lowest two eigenvalues are scaling linearly as required by condition (2.4). As $n\to\infty$ and $\gamma_n\to\gamma_\infty$, it is clear that $\bar\beta(R)\equiv R'-R$ must go to zero for $0\le R\le\frac{1}{2}$, where $\gamma_\infty$ has finite slope, and that $\bar\beta(R)$ may be nonzero only for $\frac{1}{2}\le R\le 1$ where $\gamma_\infty$ has zero slope. This clearly establishes the critical value $R_c=\frac{1}{2}$ as the point where the line of fixed points at small $R$ ends, and the transition to ordinary diffusion takes place.

For $0\le R<\frac{1}{2}$ therefore, $R'=R$ and from perturbation theory we know that $\lambda_1'$ of a system of size $2^{n-1}$ is equal to $\lambda_2$ of a system of size $2^n$. Thus $\gamma\equiv\lambda_1/\lambda_2=\lambda_1/\lambda_1'=1/\alpha(R)$ from the definition of $\alpha$ in (2.4). So $\alpha(R)=1/\gamma_\infty=2/R$ as expected [Eq. (3.4)]. For $\frac{1}{2}\le R\le 1$, $\gamma_\infty$ is just that of the equal barrier $R=1$ model, and so the long time behavior must be ordinary diffusion.

In Fig. 5 we plot $\bar\beta(R)\equiv R'-R$ as determined by the above numerical matching for the sizes considered. As expected, as $n\to\infty$, $\bar\beta(R)$ converges to a well-defined function where $\bar\beta=0$ for $0\le R<\frac{1}{2}$, while giving a flow toward $R^*=1$ for $R\ge\frac{1}{2}$. Near $R=1$, we find agreement with the decimation results of Sec. III A, $R'=\sqrt{R}$.

Finally, we have checked the $\bar\beta$ functions of Fig. 5 for consistency in matching other low-lying eigenvalue ratios $\lambda_1/\lambda_i$ for $i=3,\ldots,6$, and find good agreement. This numerically verifies the validity of our one-parameter scaling hypothesis (2.4).

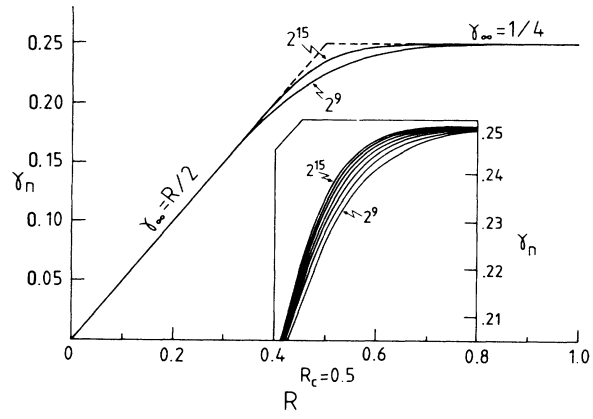


FIG. 4. Ratio of lowest two nonzero eigenvalues $\gamma_n=\lambda_1(n)/\lambda_2(n)$ vs $R$ for systems of size $2^n$. Main graph shows numerical results for sizes $2^{15}$ and $2^9$. As $n\to\infty$ the limiting curve (dashed line) is $\gamma_\infty=R/2$ for $R<R_c=\frac{1}{2}$ and $\gamma_\infty=\frac{1}{4}$ for $R>R_c$. Inset shows curves for sizes $2^n$, $n=9,\ldots,15$ on an expanded vertical scale.

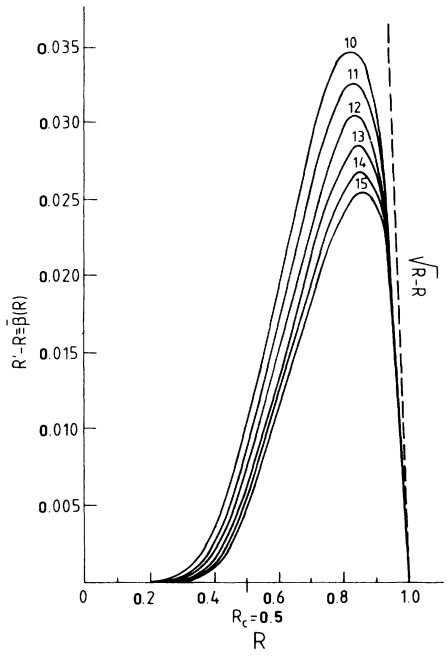


FIG. 5. Scaling functions $\bar\beta(R)$ between systems of size $2^n$ and $2^{n-1}$, i.e., $R'(2^{n-1})=R(2^n)+\bar\beta(R)$, as obtained by matching $\gamma_{n-1}(R')=\gamma_n(R)$ from the curves of Fig. 5. Curve 15, for example, results from comparison of the system of size $2^{15}$ to one of size $2^{14}$. For $R<R_c=0.5$, the curves converge to zero as $n\to\infty$, and one has a line of fixed points. For $R_c<R\le 1$, $R$ flows to $R=1$ under successive iterations. Near $R=1$, the decimation result $R'=\sqrt{R}$ is found (dashed line).

## IV. SCALING AND THE DIFFUSION CONSTANT: TRANSIENTS AND EXTERNAL FORCES

### A. Diffusion constant: renormalization approach

Having established in the previous sections a dynamic phase transition at $R_c=\frac{1}{2}$, between anomalous and ordinary diffusion, it remains an interesting question to calculate the diffusion constant $D$ of the system in the ordinary diffusive region $\frac{1}{2}\leq R\leq 1$. We define $D$ as,

$$D=\lim_{t\to\infty}\langle X^2(t)\rangle/2t \ . \tag{4.1}$$

We expect $D\to 0$ in some characteristic way as $R\to\frac{1}{2}^+$.

In principle the diffusion constant $D$ may be calculated from the scaling functions $\alpha(R)$ and $\beta(R)$ defined in Sec. II. Using the recursion relation (2.5) for the density of states $g(\lambda,R)$, and the relation (2.2) between $g(\lambda,R)$ and the autocorrelation function $P_0(t,R)$, we can derive the recursion relation for $P_0$;

$$P_0(t,R)=\tfrac{1}{2}P_0[t/\alpha(R),\beta(R)] \ . \tag{4.2}$$

For $\frac{1}{2}<R\leq 1$, we now iterate Eq. (4.2) until $R$ flows to $R^*=1$, to obtain

$$P_0(t,R)=\lim_{n\to\infty}\left[\frac{1}{2^n}P_0\left[t\prod_{i=0}^{n-1}\frac{1}{\alpha(R^{(i)})},1\right]\right] , \tag{4.3}$$

where $R^{(i)}=\beta^{(i)}(R)$ is the $i$th iterate of the RG.

But for $R^*=1$, the equal barrier model, we know $P_0(t,1)\sim t^{-1/2}$, so that $P_0(t,R)\sim(Dt)^{-1/2}$, where

$$D(R)=\prod_{i=1}^{\infty}\frac{4}{\alpha(R^{(i)})} \ . \tag{4.4}$$

Since $D$ in Eq. (4.4) sets the time scale of diffusion at $\frac{1}{2}<R\leq 1$, and the diffusion constant at $R=1$ is just unity, $D(R)$ of Eq. (4.4) is precisely the diffusion constant in the ordinary diffusive region.

In order to calculate $D(R)$ from (4.4) we need to know the scaling functions $\beta(R)$ and $\alpha(R)$ accurately, particularly near the critical point $R_c=\frac{1}{2}$. The numerical methods discussed here were not sufficiently accurate to do this. However the analytic recursion relations derived by the decimation scheme of Maritan and Stella[22] can be used successfully to calculate $D(R)$, as discussed elsewhere.[23] We turn instead to an easier method.

### B. Diffusion constant: standard treatment

A very general result[14,15] proved by Zwanzig[16] shows that for any one-dimensional arrangement of $N$ barriers, the diffusion constant is simply related to the hopping rates by

$$\frac{1}{D}=\frac{1}{N}\sum_{k=1}^{N}\frac{1}{W_{k,k+1}} \ . \tag{4.5}$$

In our models, for a system of size $N=2^n$ there are $2^{n-m-1}$ barriers of rate $R^m$. So the sum becomes

$$\frac{1}{D}=\tfrac{1}{2}\sum_{m=0}^{n}\frac{1}{(2R)^m} \ . \tag{4.6}$$

For $n\to\infty$ the geometric series (4.6) diverges for $R<R_c=\frac{1}{2}$, i.e., $D=0$, while for $R>R_c$ one obtains

$$D(R)=2(R-\tfrac{1}{2})/R \ . \tag{4.7}$$

Therefore the diffusion constant vanishes linearly as $R\to R_c^+$.

This approach allows us to make a more general statement. Since the sum (4.5) is independent of the ordering of the barriers, there will be a dynamic phase transition from ordinary to anomalous diffusion as $R$ decreases through $R_c=\frac{1}{2}$, for any spatial arrangement of barriers, provided they have the same distribution of rates as in our hierarchical model. One may now ask whether the autocorrelation function exponent $x(R)$, see Eq. (3.5), in the anomalous region $R<R_c$ depends in general on the spatial arrangement, or just on the rate distribution as in the case of $D(R)$. For the case of randomly positioned barriers exactly the same results (3.5) for $x(R)$ were found in an explicit calculation by Alexander *et al.*[14] For the more general case, we believe that the scaling arguments presented below in Sec. IV C show $x(R)$ to remain equal to our result (3.5) for all chains which possess a reasonable $N\to\infty$ limit.

### C. Anomalous diffusion from scaling

Finally, we can use the result (4.6) to calculate the autocorrelation function exponent $x(R)$ in the anomalous region via the following scaling argument.[26] For a system of finite[27] size $N=2^n$, the diffusion constant is finite and given by (4.6) as

$$D(N)=\frac{1-(1/2R)}{1-(1/2R)^n}\sim N^{1+\ln R/\ln 2} \ . \tag{4.8}$$

The time it takes a particle to move a mean-square distance of order $N$, the size of the system, is thus given by

$$N^2\sim D(N)t \ . \tag{4.9}$$

Substituting (4.8) in the expression (4.9) and rearranging powers of $N$ gives

$$N^2\sim t^{2\ln 2/(\ln 2-\ln R)} \ . \tag{4.10}$$

This, combined with the scaling relation (2.3) connecting the mean-square distance to the autocorrelation function, reproduces the anomalous exponent found in (3.5).

We have verified Eq. (3.5) and (3.8) by doing numerical simulations for several values of $R$ both above and below the transition $R_c=\frac{1}{2}$. A discrete-time version of the master equation was used:

$$\begin{aligned}P_k(t+\Delta t)-P_k(t)=&(W_{k+1,k}\,\Delta t)P_{k+1}(t)\\&+(W_{k-1,k}\,\Delta t)P_{k-1}(t)\\&-[(W_{k,k+1}+W_{k,k-1})\Delta t]P_k(t) \ .\end{aligned} \tag{4.11}$$

The initial position of a particle was chosen randomly in the central third of a long chain, and a random walk was generated. At each time step a random number $0<r<1$ was generated, and a move decided according to

$$\Delta k = \begin{cases} -1, & r < W_{k,k-1}\,\Delta t \\ +1, & r > 1 - W_{k,k+1}\,\Delta t \\ 0, & \text{otherwise} . \end{cases} \tag{4.12}$$

Since one must have $W_{k,k-1}\,\Delta t < 1 - W_{k,k+1}\,\Delta t$, we used the largest possible value $\Delta t$ can take, i.e., $\Delta t = 1/(1+R)$. Ensembles of more than 5000 such walks were generated to calculate the average distance squared, $\langle X^2(t)\rangle \equiv \langle [k(t)-k(0)]^2\rangle$, averaging initial positions $k(0)$ over a large (albeit finite) number of sites. Boundary effects were treated by allowing addition of sites beyond the boundary, if the diffusing particle reaches it. In practice this happened extremely rarely.

Our results, $\ln\langle X^2(t)\rangle$ versus $\ln t$ for two values $R = 0.7 > R_c$ and $R = 0.2 < R_c$ are shown in Figs. 6(a) and 6(b). The asymptotic behaviors agree with those predicted in Secs. III and IV B and IV C. For long times, the slope of Fig. 6(a) is unity, corresponding to ordinary diffusion, while the $\ln t = 0$ intercept is just $\ln D$, $D = 0.57$ [as compared to the prediction from Eq. (4.7), $D = 0.572$]. For Fig. 6(b), the slope is 0.61 compared to the predicted value $2\ln 2/(\ln 2 - \ln R) = 0.60$.

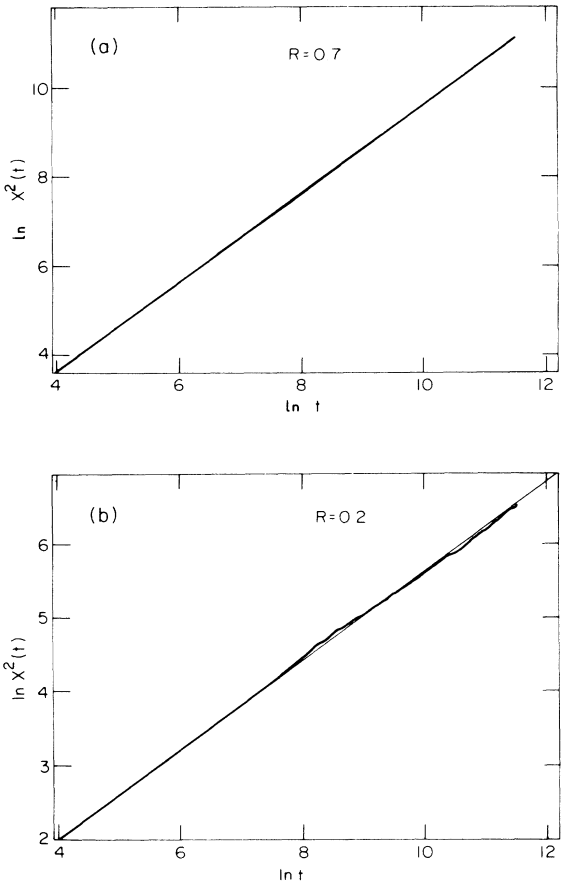


FIG. 6. Results of numerical simulation for displacement $\langle X^2(t)\rangle \equiv \langle [k(t)-k(0)]^2\rangle$ vs time $t$, on a log-log scale. (a) is for $R = 0.7 > R_c$; the slope as $t \to \infty$ is unity, as expected for ordinary diffusion. The diffusion constant, determined numerically from the $\ln t$ intercept is $D = 0.57$, as compared to the theoretical value 0.572 from Eq. (4.7). (b) is for $R = 0.2 < R_c$, the slope is 0.61, corresponding to anomalous diffusion, and is in good agreement with the theoretical value 0.60, as obtained from Eqs. (2.3) and (3.5).

### D. Transient response

Until now we have only treated the asymptotic ($t \to \infty$) behavior of the hierarchical chain. In this section we turn to consider the transient behavior at intermediate times. Our purpose is to predict $\langle X^2(t)\rangle = \langle (k(t)-k_0)^2\rangle$, the average squared displacement as a function of time, where we average over initial position $k_0$.

Motion at intermediate times is conveniently described in terms of a local time dependent diffusion constant $\tilde{D}(t)$, defined by

$$\langle X^2(t)\rangle = 2\tilde{D}(t)t . \tag{4.13}$$

Given $\tilde{D}(t)$, one can calculate the average displacement $\langle X^2(t)\rangle$ as above. Equivalently, we can choose to define a local, length-scale-dependent diffusion constant $\tilde{D}(X)$. The time required to move the mean-square distance $X \equiv (\langle X^2\rangle)^{1/2}$ is then just

$$t(X) = X^2/2\tilde{D}(X) . \tag{4.14}$$

Clearly $\tilde{D}(X)$ is simply related to $\tilde{D}(t)$ by $\tilde{D}(X) = \tilde{D}(X(t))$.

We now make the following ansatz about the function $\tilde{D}(X)$, based on the success of the scaling method of Sec. IV C. We assume that $\tilde{D}(X)$ must scale with $X$ in an hierarchical way, representative of the hierarchical structure of our chain. That is, we *assume* that at time $t$, the system has effectively sampled barriers in the chain, only up to some level of the hierarchy $n(t)$. That is, only barriers of rates $R^l$, $l < n(t)$, have as yet played an important role. The mean-square distance $X$ traversed in this time, is just proportional to the distance $N = 2^{n(t)}$ required to sweep out these barriers. We can thus compute $\tilde{D}(X)$, via Eq. (4.5), by averaging the inverse hopping rates of the barriers up to this level $n$ of the hierarchy. This calculation has already been done in Eq. (4.8), where we have written an explicit equation for $D(N)$, the diffusion constant for a chain of length $N = 2^n$, containing barriers up to the $n$th level of the hierarchy. Thus the $\tilde{D}(X)$ defined by Eq. (4.14), can be expressed in terms of $D(N)$ of Eq. (4.8);

$$\tilde{D}(X) = D(N = X/f), \quad D(N) = \frac{1 - 1/2R}{1 - (1/2R)^n} , \quad N = 2^n \tag{4.15}$$

where $f$ is an unknown proportionality constant. Equations (4.14) and (4.15) thus completely specify the transient behavior of the system, and enable us to directly calculate $t(X)$.

We have tested this scaling ansatz by checking against numerical simulations. The details of the simulation method have already been presented in the preceding section. In Fig. 7(a) we present results for $\langle X^2\rangle$ versus $t$ for

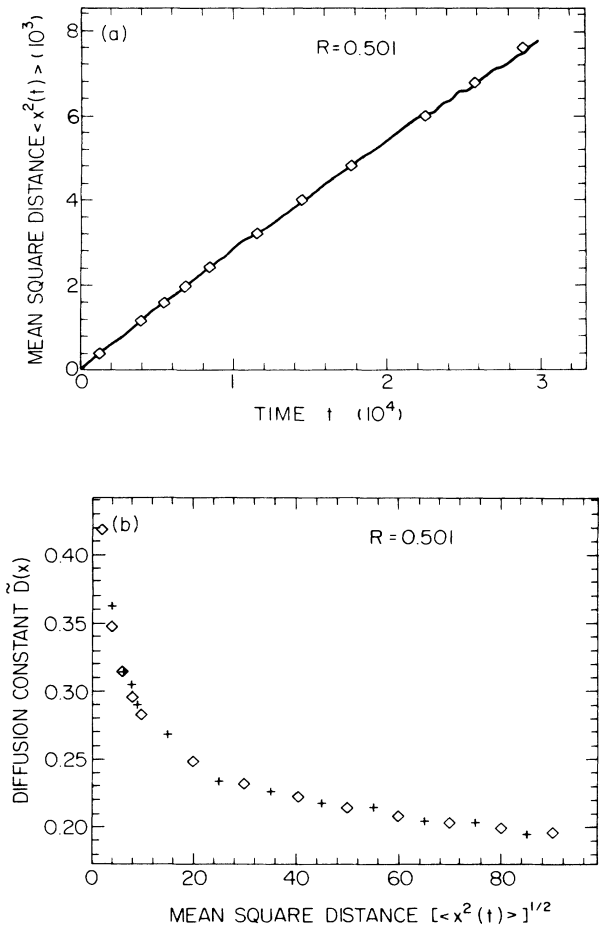


FIG. 7. (a) Mean-square displacement $\langle X^2(t)\rangle$ vs time, for $R=0.501>R_c$. The solid line represents results of numerical simulation, compared with the theoretical prediction (diamonds) based on Eqs. (4.14) and (4.15) with $f=0.29$. (b) $\tilde{D}(X)$ vs $X$, as obtained from simulations (crosses), using Eq. (4.14), compared with the analytic expression (diamonds) from (4.15). The parameter $f=0.29$ was obtained from best fit.

a value of the parameter $R=0.501>R_c$. We have chosen a value close to $R_c$ in order to have the largest transient effects. The solid line represents the numerical data from the simulation, while the diamonds represent our theoretical prediction as computed from Eqs. (4.14)–(4.15). Excellent agreement is obtained for a value of $f=0.29$. In Fig. 7(b), we plot $\tilde{D}(X)$ versus $X$, in order to highlight the transient effects in Fig. 7(a). The crosses represent values $\tilde{D}(X)=\langle X^2(t)\rangle/2t$ obtained from the simulation data, while the diamonds are the values computed from Eq. (4.15). The transient effects are now more clearly presented, with $\tilde{D}(X)$ decaying toward its asymptotic value (4.7) as $X\to\infty$. Agreement between simulation and our ansatz, obtained by best fitting a single parameter $f$, remains excellent. Thus the validity of our ansatz is verified.

Similar agreement is found for $R=0.499<R_c$. The only difference is that for $R<R_c$ the asymptotic value of $\tilde{D}(X)$ vanishes. Having established the validity of Eqs. (4.14)–(4.15) for the transient behavior, we can ask what is the time scale on which the system crosses over to its asymptotic long-time limit. From Eq. (4.8) we see that $D(N(t))$ approaches its asymptotic limit *algebraically*. Hence no sharp crossover time exists. For $R>R_c$, we can define instead a time $\tau_\epsilon$ which is the time it takes for the diffusion constant to reach its asymptotic value to within a fraction $\epsilon$, i.e., $D(N(\tau_\epsilon))=D(\infty)(1+\epsilon)$. From Eq. (4.8) for $D(N)$ we have

$$n(\tau_\epsilon)=-\ln\epsilon/\ln(2R),\quad N=2^n\ . \tag{4.16}$$

Combining this with Eq. (4.14) then gives $\tau_\epsilon\sim N^2/D(N)\sim 2^{2n}/D(\infty)$ or

$$\tau_\epsilon\sim\frac{e^{-\ln 2\ln\epsilon/(R-R_c)}}{R-R_c}\quad\text{as } R\to R_c^+\ . \tag{4.17}$$

This relaxation time $\tau_\epsilon$ therefore obeys a Vogel-Fulcher law near the transition. Similarly, for $R<R_c$, we can define $\tau_\epsilon$ as the time it takes for the diffusion constant to reach within a fraction $\epsilon$ of its asymptotic scaling behavior, i.e., $D(N(\tau_\epsilon))=D(N(\infty))(1+\epsilon)$. By $D(N(\tau_\epsilon))$ and $D(N(\infty))$ we mean the exact and large $N$ scaling expressions for $D$, as given by the middle and right most terms in Eq. (4.8), respectively. This $\tau_\epsilon$ thus measures deviations from the asymptotic behavior (4.10). Again one finds $n(\tau_\epsilon)=\ln\epsilon/\ln(2R)$ and so a similar Vogel-Fulcher–type law is obtained. Note that since $R$ depends on temperature $T$, linearization of $R(T)$ near $T_c$ [defined by $R(T_c)=R_c$] yields the conventional Vogel-Fulcher form.

### E. Response to an external force

In this subsection we study motion in the presence of the hierarchical barriers described above, *and* a *uniform external force*. Since the diffusion constant is proportional to the mobility (Einstein relation), one expects the mobility to vanish for $R<R_c$. Hence in this anomalous regime the net average velocity of the system vanishes; no current is generated in (linear) response to the external force.

The external force can be represented by breaking the (left-right) symmetry of the transition rates, e.g., $W_{k,k+1}\neq W_{k+1,k}$. We assume that the rates $W_{k,k+1}$ are determined by thermally activated hopping over energy barriers. The uniform force $F$ is derived from a potential of constant slope, and hence for all $k$

$$\begin{aligned} &W_{k,k+1}=aW_{k+1,k}\ ,\\ &a=e^{-\Delta E/k_BT}=e^{-Fd_0/k_BT}\ , \end{aligned} \tag{4.18}$$

where $d_0$ is the lattice spacing.

The master equation takes the form

$$\begin{aligned} \frac{dP_k}{dt}&=W_{k+1,k}P_{k+1}(t)+W_{k-1,k}P_{k-1}(t)\\ &\quad-(W_{k,k+1}+W_{k,k-1})P_k(t)\ . \end{aligned} \tag{4.19}$$

The steady-state solutions $P_k^{ss}$ is obtained by setting $dP_k^{ss}/dt=0$. The explicit solution can be obtained using

the methods of Van Kampen[20] and Derrida.[27] The steady state velocity is given by

$$V^{ss}=\frac{\sum_{k=1}^{N}(W_{k,k+1}-W_{k,k-1})P_k^{ss}}{\sum_{k=1}^{N}P_k^{ss}} . \tag{4.20}$$

If we now use the hierarchical rates of the last sections for $W_{k+1,k}$ and the solution[20,26] for $P_k^{ss}$, we obtain in the $N\to\infty$ limit

$$V^{ss}(R)=(a-1)D(R) , \tag{4.21}$$

with $D(R)$ given by (4.5). For small forces, $Fd_0 \ll k_B T$, the linear response, i.e., Einstein relation

$$\mu\equiv\frac{V^{ss}(R)}{F}=\frac{D(R)}{k_B T}d_0 \tag{4.22}$$

is found.

For $R>R_c$, $D(R)>0$ and finite mobility (or a constant steady state) velocity $V^{ss}$ is obtained. This means linear drift $\langle X(t)\rangle = V^{ss}t$. For $R<R_c$ the response to a uniform external force is *not* a constant steady state current. Rather, the motion in the anomalous regime has the form

$$\langle X(t)\rangle \sim t^{\beta},\quad \beta=-\ln 2/\ln R . \tag{4.23}$$

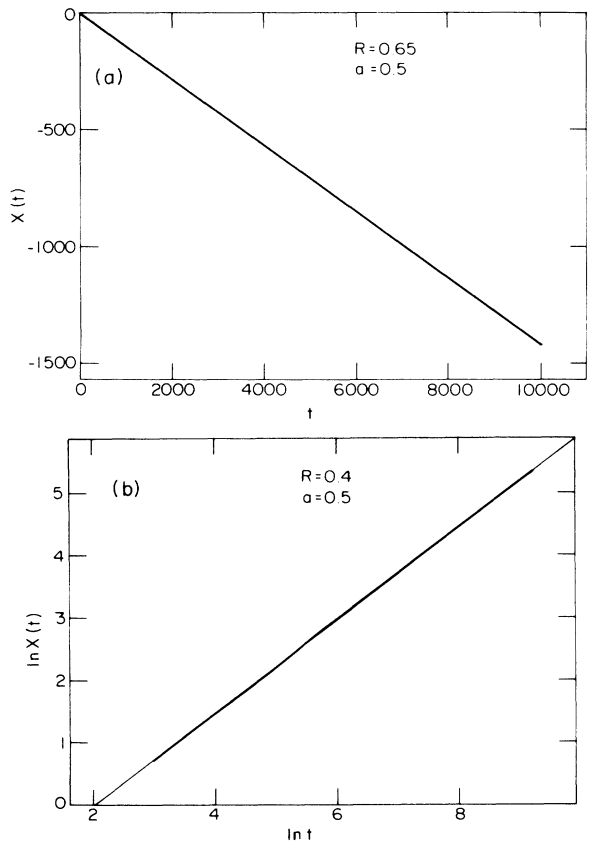


FIG. 8. Results of numerical simulations for displacement $\langle X(t)\rangle=\langle k(t)-k(0)\rangle$ vs time $t$, in the presence of a uniform applied force $F$, where $a\equiv\exp(-Fd_0/k_B t)=0.5$. (a) is for $R=0.65>R_c$; the asymptotic velocity from the simulation is $v=0.235$ as compared to 0.230 as calculated from Eq. (4.21). (b) is for $R=0.4<R_c$; the asymptotic behavior is governed by the exponent $\beta$ [Eq. (4.18)] which is found in the simulation to be 0.75 as compared to 0.756 as calculated from Eq. (4.23).

We calculate $\beta$ by a method similar to that of Secs. IV B and IV C. We first consider a finite system; from (4.21) and (4.8) we have

$$V(N)\propto D(N)\sim N^{\ln R/\ln 2+1} . \tag{4.24}$$

Hence the time needed to traverse distance $N$ is $t(N)$, given by

$$t(N)=N/V(N)\sim N^{-\ln R/\ln 2} , \tag{4.25}$$

and from this we finally get $\beta$ of (4.23). Hence in the normal diffusive regime ($R>R_c$) the linear response to a constant external force is a steady-state current, with constant velocity. The mobility is proportional to $D$ (Einstein relation). In the anomalous, subdiffusive regime mobility and diffusion constant vanish; the system responds to the external force by a nonlinear drift, given by (4.23).

The predictions (4.21) and (4.23) were confirmed in numerical simulations, the details of which were described in Sec. IV C. Ensembles of more than 5000 such walks were generated to yield $\langle X(t)\rangle\equiv\langle k(t)-k(0)\rangle$. The results were found to be in excellent agreement with (4.21) for $R>R_c$ or (4.23) for $R<R_c$. Deviations, of order 2%, are due to the fact that averaging over initial positions was taken over a subset (5000 out of $10^5$) of the allowed sites.

Representative simulations are shown in Figs. 8(a) and 8(b), for $R=0.65>R_c$ and $R=0.4<R_c$, respectively, using $a=0.5$ for both. For $R=0.65$ the measured and calculated velocities are $V=0.235$ and 0.240, respectively. For $R=0.4$ the exponent $\beta$ was measured (predicted) to be 0.75 (0.756).

## V. HIGHER DIMENSIONS

We consider now the generalization of our hierarchical model to higher dimensions. The case for $d=2$ is shown in Fig. 9. We will focus here on $d=2$ for description

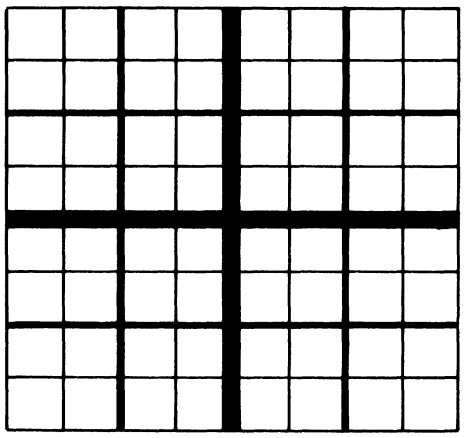

FIG. 9. Hierarchical model in two dimensions. The system when in cell $\mathbf{r}$ can hop only to its nearest-neighbor cells, $\mathbf{r}\pm\hat{\mathbf{x}}$ and $\mathbf{r}\pm\hat{\mathbf{y}}$. The height of the barriers between cells is proportional to the thickness of the lines in the figure. Moving along any column or row one sees the same sequence of barriers as in the one dimensional model of Fig. 1. The highest central barriers (thickest lines) split the system into four quadrants which form the basis of the perturbation theory of Eq. (5.1).

sake, but the generalization to arbitrary $d$ is trivial. In Fig. 9, the thicker the line, the higher the barrier it represents. Moving along the system down any column or across any row, one sees the same sequence of barriers as in the one dimensional model of Fig. 1. The master equation connects nearest-neighbor cells; i.e., cell $\mathbf{r}$ is connected to $\mathbf{r}\pm\hat{\mathbf{x}}$, $\mathbf{r}\pm\hat{\mathbf{y}}$, etc. The master-equation matrix $\underline{M}(n)$, for a system of length $2^n$, factors in a similar way as the one-dimensional case discussed in Sec. III B [see Eq. (3.9)].

$$\underline{M}(n)=\underline{M}^{2^d}(n-1)+\underline{M}_1(n)\ , \tag{5.1}$$

where the first term is just the decoupled direct product of the $2^d$ subsystems of length $2^{n-1}$, and $\underline{M}_1$ is the coupling between them due to the tallest barrier connecting cells along the common edges of these subsystems. In terms of the two dimensional example of Fig. 9, $\underline{M}^{2^d}(n-1)$ contains the matrix elements describing the hopping among cells contained *within* each of the four largest quadrants (assuming an infinite barrier at the quadrant edges); while $\underline{M}_1(n)$ contains the matrix elements describing the hopping *between* quadrants across the tallest barrier (thickest line) separating them. $\underline{M}_1(n)$ is of order $R^{n-1}$.

In two dimensions, let $xy$ and $x'y'$ denote sites on the lattice. Then $\underline{M}_1(n)$ is a $2^{2n}\times 2^{2n}$ matrix, whose elements are most naturally characterized by two indices; $[\underline{M}_1(n)]_{xy,x'y'}$ represents that matrix element connecting site $xy$ to site $x'y'$. The only nonvanishing elements of $\underline{M}_1(n)$ are associated with the internal boundary sites of the four largest quadrants; i.e., a site $xy$, on the boundary $B$ of one quadrant, from which one can hop to a site $x'y'$, on the boundary $B'$ of a different quadrant. Labeling these internal boundaries $B_i$, $i=1,2,3,4$, we have

$$[\underline{M}_1(n)]_{xy,x'y'}=\begin{cases} R^{n-1}, & xy=x'y'\in B_i \text{ any } i \\ -R^{n-1}, & xy\in B_i,\ x'y'\in B_j,\ i\neq j,\ xy \text{ and } x'y' \text{ nearest neighbors} \\ 0, & \text{otherwise}\ . \end{cases} \tag{5.2}$$

As in the one-dimensional case, each eigenvector $\psi(n-1)$ of $\underline{M}(n-1)$, with eigenvalue $\lambda$, must either be symmetric or antisymmetric with respect to reflection, in any one of the $d$ directions about the tallest barrier in the center. Thus we can construct from each $\psi(n-1)$ the $2^d$ degenerate eigenvectors, with eigenvalue $\lambda$, of $\underline{M}^{2^d}(n-1)$, which form the zeroth-order approximates to the eigenvectors of $\underline{M}(n)$. These are just the symmetric and antisymmetric direct products of $\psi(n-1)$. In two dimensions they are

$$\begin{aligned} \psi_1^{(0)}(n)&=\begin{bmatrix}\psi & \psi\\ \psi & \psi\end{bmatrix},\quad \psi_2^{(0)}(n)=\begin{bmatrix}\psi & \psi\\ -\psi & -\psi\end{bmatrix}, \\ \psi_3^{(0)}(n)&=\begin{bmatrix}\psi & -\psi\\ \psi & -\psi\end{bmatrix},\quad \psi_4^{(0)}(n)=\begin{bmatrix}\psi & -\psi\\ -\psi & \psi\end{bmatrix}. \end{aligned} \tag{5.3}$$

These zeroth-order approximates have a reflection symmetry determined by the original symmetry of $\psi(n-1)$, and the symmetry of the direct product taken. Thus for example, if $\psi(n-1)$ is symmetric with respect to reflection in $\hat{\mathbf{x}}$ and antisymmetric with respect to reflection in $\hat{\mathbf{y}}$, then the product $\psi_2^{(0)}$ of Eq. (5.3) will be symmetric in $\hat{\mathbf{x}}$ and symmetric in $\hat{\mathbf{y}}$, while the product $\psi_1^{(0)}$ will be symmetric in $\hat{\mathbf{x}}$ and antisymmetric in $\hat{\mathbf{y}}$, etc.

The splitting of each eigenvalue $\lambda$ of $\underline{M}(n-1)$ into $2^d$ new eigenvalues of $\underline{M}(n)$ is given to lowest order by the diagonal matrix elements (off-diagonal elements vanish by symmetry)

$$\delta\lambda_j^{(1)}(n)=\langle\psi_j^{(0)}(n)\,|\,\underline{M}_1(n)\,|\,\psi_j^{(0)}(n)\rangle\ , \tag{5.4}$$

where $j=1,\ldots,2^d$. We now evaluate this matrix element, to lowest order in $R$. In two dimensions we consider for example

$$\psi_j^{(0)}(n)=\frac{1}{(2^{dn})^{1/2}}\begin{bmatrix}\cdots & x & 1 & -1 & -x & \cdots\\ \cdots & x & 1 & -1 & -x & \cdots\\ \cdots & x & 1 & -1 & -x & \cdots\\ \cdots & x & 1 & -1 & -x & \cdots\end{bmatrix}, \tag{5.5}$$

i.e., a function symmetric in $\hat{\mathbf{y}}$ and antisymmetric in $\hat{\mathbf{x}}$. To lowest order in $R$, all elements of $\psi_j^{(0)}$ are $\pm 1$, with an overall normalization of $1/2^{dn/2}$.

To evaluate (5.4) we just consider the function

$$\tilde{\psi}=\underline{M}_1(n)\psi_j^{(0)}(n)\ ,$$

with $\underline{M}_1$ as given in (5.2). The only nonzero elements of $\tilde{\psi}$ are at $xy\in B_i$. Say $x'y'$ is the nearest neighbor to which $xy$ is connected by $\underline{M}_1$. The $xy$ element of $\tilde{\psi}$ will be nonzero only if the signs of $\psi_j^{(0)}$ on $xy$ and on $x'y'$ are not the same; that is, $\tilde{\psi}_{xy}\neq 0$ only if $\psi_j^{(0)}$ is antisymmetric with respect to the reflection that maps $xy\leftrightarrow x'y'$.

Hence, for our example $\psi_j^{(0)}$ of (5.5) we get

$$\tilde{\psi}=(R^{n-1}/2^{dn/2})\begin{bmatrix}0 & 2 & -2 & 0\\ 0 & 2 & -2 & 0\\ 0 & 2 & -2 & 0\\ 0 & 2 & -2 & 0\end{bmatrix}. \tag{5.6}$$

To obtain (5.4), the linear product $\langle\psi_j^{(0)}\,|\,\tilde{\psi}\rangle$ has to be taken; this will yield [see Eqs. (5.5) and (5.6)]

$$\langle\psi_j^{(0)}\,|\,\tilde{\psi}\rangle=R^{n-1}\times 2^{-dn}\times 4\times 2^{(d-1)n}\ . \tag{5.7}$$

The last factor of $2^{(d-1)n}$ comes from the fact that in $d$ dimensions there are $2^{(d-1)n}$ sites along a single boundary surface that separates the system into two halves.

For general $d$ and any $\psi_j^{(0)}$, we proceed in a similar

manner. If the initial $\psi_j^{(0)}$ is antisymmetric about $d'$ out of the $d$ possible directions in $d$ dimensions, then the above arguments hold for each antisymmetric direction and the result is simply multiplied by $d'$. We thus have in general that the splittings of the new eigenvalues to lowest order in $R$ are

$$\delta\lambda_{d'}^{(1)}(n)=2(R/2)^{n-1}d' , \tag{5.8}$$

where each $\delta\lambda_{d'}^{(1)}$ has degeneracy $d!/(d'!)(d-d')!$, i.e., the number of ways to select the $d'$ antisymmetric directions from the $d$ possibilities. Note that for that particular product (5.3) which gives a $\psi_j^{(0)}(n)$ symmetric in all directions, i.e., $d'=0$, $M_1\psi_j^{(0)}=0$, so $\delta\lambda=0$, and this $\psi_i^{(0)}(n)$ is an exact eigenvalue of the new system. Thus as in one dimension, all eigenvalues of the system of size $2^{n-1}$ remain eigenvalues of the system of size $2^n$, with $2^d-1$ new eigenvalues splitting off from each old one, each splitting of order $R^{n-1}$ as in Eq. (5.8).

To higher order in perturbation theory, we can again argue that the recursive nature of the matrices produces an expression of the form (3.12) and so as $n\to\infty$ we again find that the eigenvalues scale with the same coefficient, $\lambda_{d'}(n-1)/\lambda_{d'}(n,R)\equiv\alpha(R)$, where $\alpha(R)=2/R$ as in one dimension. Thus we again have a line of fixed points $R'=R$.

In $d$ dimensions the recursive relation for the density of states is trivially found to be modified as

$$g(\lambda,R)=\frac{\alpha(R)}{2^d}g(\alpha(R)\lambda,\beta(R)) \tag{5.9}$$

and so identical arguments as presented in Sec. III give for the autocorrelation function along the fixed line,

$$P_0(t,R)\sim t^{-x(R)},\quad x(R)=\frac{d\ln 2}{\ln 2-\ln R} . \tag{5.10}$$

Thus we have anomalously slow diffusion with an exponent which is just the one dimensional result, multiplied by the dimensionality $d$. Since the exponent associated with ordinary diffusion in $d$ dimensions is simply $x=d/2$, if we assume $x(R)$ to be a continuous function of $R$ through the transition, as in one dimension, we again get $R_c=\frac{1}{2}$.

We can demonstrate the validity of this last assumption regarding the continuity of $x(R)$, by just noting that if $\psi_k$ is an eigenvector of $M_{kk'}$ for the $1d$ problem, with the eigenvalue $\lambda$, then we can construct an eigenvector of the $d$ dimensional problem by letting $\psi_{k_1,k_2,\ldots,k_d}=\psi_{k_1}$ for all $k_2,k_3,\ldots,k_d$ (where $k_1,k_2,\ldots,k_d$ are the site coordinates), i.e., we just let $\psi$ vary as in the $1d$ case in one particular direction, and copy it identically in all the transverse directions. The resulting eigenvalue is the same $\lambda$ as for the $1d$ $\psi_k$. The subset of eigenvalues of the $d$-dimensional problem obtained this way, therefore scales in exactly the same way as the $1d$ problem and so we get the same functions $\beta(R)$ and $\alpha(R)$. The perturbation result tells us that *all* eigenvalues must scale this same way along the fixed line, and if we assume the same is true in the ordinary diffusive region, we therefore must have $R_c=\frac{1}{2}$.

Thus the generalization to $d$ dimensions produces no qualitatively new results. There is again a dynamic phase transition at $R_c=\frac{1}{2}$ between anomalous and ordinary diffusion, and the autocorrelation exponent $x(R)$ is just $d$ times the one dimensional value. For a $d$-dimensional problem in which the barriers are placed in a manner other than our spatially hierarchical way, such as randomly, the results are expected to be more complicated.

## VI. SUMMARY AND DISCUSSION

We have solved the problem of diffusion in the presence of a one-dimensional hierarchical set of barriers (Fig. 1), where the hopping rates from one level of the hierarchy to the next scale with a constant factor $0\le R\le 1$. We find a phase transition in the asymptotic long-time dynamics at $R_c=\frac{1}{2}$. For $R_c\le R$ we have ordinary diffusion; the autocorrelation function behaves as $P_0(t)\sim t^{-1/2}$ and the mean-square distance as $\langle X^2(t)\rangle\sim Dt$, where the diffusion constant vanishes linearly as $R\to R_c^+$. For $R<R_c$ we have anomalously slow diffusion. The autocorrelation function behaves as $P_0(t)\sim t^{-x(R)}$, where $x(R)=\ln 2/(\ln 2-\ln R)\le\frac{1}{2}$ is a continuous function of $R$ and equals $\frac{1}{2}$ at $R=R_c$. We solved the problem in the presence of a constant external force. The Einstein relation was found to hold, producing a steady-state current in the diffusive regime, and an anomalous response in the subdiffusive regime. We also found analytical estimates for the time it takes for the asymptotic (long-time) behavior to set in. We have considered a generalized hierarchical structure in arbitrary dimensions $d$ and conclude that the same behavior as in the $1d$ case remains; a transition occurs at $R_c=\frac{1}{2}$ only autocorrelation function exponents are now just $dx(R)$. For the $1d$ case we have also considered different spatial orderings of the barriers. We find that, provided the distribution of hopping rates is the same as in our hierarchical model, there remains a transition at $R_c=\frac{1}{2}$, and that the long-time behavior is identical in the ordinary diffusive region for all possible spatial orderings. For the particular case of *random* ordering,[14] the autocorrelation exponent in the anomalous region $R<R_c$ is also identical to our hierarchical model. These observations suggest that the type of transition we find may be of a more general nature than just describing the particular model considered here.

Although the problem we have considered is a single-particle problem, the scenario for the dynamic transition we find here may be of relevance for certain many-body thermodynamic systems. For example, dynamics of spin systems can be viewed as a random walk in *phase space*. Usually the possible transitions are severely restricted (single spin-flip, or some finite number of spins can be flipped in any one time step). Such restrictions force the system, in order to reach some point of low energy, to transverse points with high energy. This produces large barriers between low-lying states. Even though phase space is high dimensional, in some circumstances[28,29] dynamics may be dominated by a small number of phase-space trajectories, and hence our model may have applicability.

In particular, we wish to mention the possible connection between dynamical transitions as in our model, and behavior in glassy systems.[30] Our model, consisting of a

single particle, has no interesting equilibrium thermodynamic behavior. Nevertheless we found a diverging time scale $1/D$ at a well-defined value of our parameter $R_c$. Similarly, the glassy transition is often characterized as being a purely dynamic phenomenon;[31] a time scale diverges causing the system to "freeze" (i.e., have a vanishing self-diffusion constant[32]), at a temperature where the correlation length $\xi$ remains finite (and so has no divergent equilibrium behavior). A scenario for such a purely dynamic phase transition in a many-body system is sketched in Fig. 10, in terms of the flows of the system under a dynamic renormalization group. We imagine that the parameter space for the system is described by two variables; the equilibrium temperature variable $T$, and some dynamic variable $R$. The physical many-body system is described by a trajectory $R_0(T)$ in this plane. Under iterations of the RG however the system will flow off the trajectory, into the $(R,T)$ plane. Since there is no equilibrium phase transition in the system at finite $T$ (i.e., $\xi$ finite), the system must flow to infinite temperature, i.e., somewhere on the line $T=\infty$. Along the line at infinite temperature, the system, as expressed in suitable coordinates, should separate into noninteracting single-particle pieces. If one of these single-particle problems has a dynamic phase transition, for example of the sort discussed in this paper and sketched in Fig. 10, then the original physical system will also have a dynamic transition at the point on the trajectory $R_0(T)$ which crosses the separatrix between flows to the different dynamical fixed points on the line $T=\infty$. Such a point will be characterized by a diverging time scale, but smooth equilibrium correlation functions.

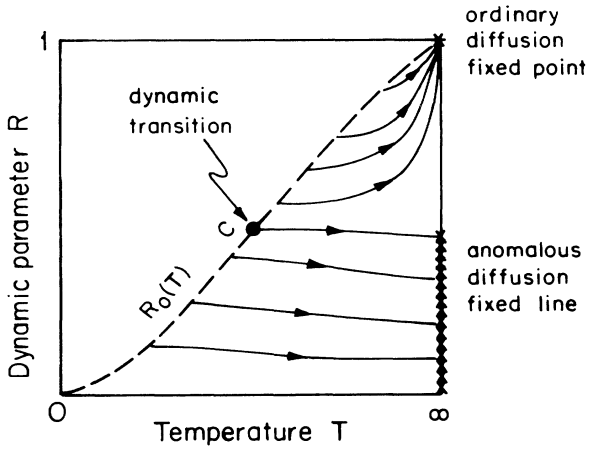


FIG. 10. Schematic renormalization-group flow diagram for a glassy transition. The $T$ axis is the thermodynamic variable temperature, while the $R$ axis represents some dynamic parameter. The physical system is described by an initial trajectory $R_0(T)$ (dashed line). Under the RG the system flows off this initial trajectory into the $(R,T)$ plane. Since there is no thermodynamic phase transition, all points flow to the $T=\infty$ line. If at $T=\infty$, there is a dynamic transition in the $R$ variable, the physical system will have a dynamic transition at the point $C$ which is the intercept of the initial trajectory with the seperatrix for flows into the different fixed points at $T=\infty$.

Although we are far from producing a physical many-body model with an explicit flow diagram as in Fig. 10, these arguments suggest that it is of direct interest to study the simpler possible single-particle dynamic transitions.[29] All many-body cases such as Fig. 10 must fall into one of these single-particle classes.

## ACKNOWLEDGMENTS

We thank A. Aharony, S. Alexander, J. Gubernatis, R. Landauer, M. Kerszberg, W. Kinzel, and D. Mukamel for suggestions, discussions and correspondence. This research was partially supported by grants from the Israel Academy of Science and Humanities and the U.S.-Israel Binational Science Foundation.

## APPENDIX A

In this appendix we rederive several relationships concerning the autocorrelation function $P_0(t)$. First we prove Eq. (2.2) connecting $P_0(t)$ to the density of states $g(\lambda)$

$$P_0(t)=\int_0^\infty g(\lambda)e^{-\lambda t}d\lambda \ . \tag{A1}$$

Let $\psi_{\lambda_i}(k)$ be an eigenvector of the matrix $M_{k,k'}$ with eigenvalue $\lambda_i$, where we choose normalization

$$\sum_k |\psi_{\lambda_i}(k)|^2=1 \ . \tag{A2}$$

Since $M$ is symmetric, the set $\{\psi_\lambda\}$ form an orthogonal basis for expanding any vector $P(k)$. For the initial probability distribution $P(k,t=0)$ we expand

$$P(k,0)=\sum_{\lambda_i}\sum_{k'}P(k',0)\psi^*_{\lambda_i}(k')\psi_{\lambda_i}(k) \ . \tag{A3}$$

It is now straightforward to see, by direct substitution into the master equation (2.1), that the solution for the time evolution of $P(k,t)$ is simply

$$P(k,t)=\sum_{\lambda_i}\sum_{k'}P(k',0)\psi^*_{\lambda_i}(k')\psi_{\lambda_i}(k)e^{-\lambda_i t} \ . \tag{A4}$$

If we take as the initial condition $P(k,0)=\delta_{k,k_0}$, i.e., the particle starts off at site $k_0$, then the probability to remain at $k_0$ after time $t$ is simply

$$P(k_0,t)=\sum_{\lambda_i}\psi^*_{\lambda_i}(k_0)\psi_{\lambda_i}(k_0)e^{-\lambda_i t} \ . \tag{A5}$$

Averaging (A5) over this initial $k_0$, and noting the normalization conduction (A2) for $\psi_{\lambda_i}$, gives for the autocorrelation function,

$$P_0(t)\equiv\frac{1}{N}\sum_{k_0}P(k_0,t)=\frac{1}{N}\sum_{\lambda_i}e^{-\lambda_i t} \ . \tag{A6}$$

Noting the definition of the density of states $g(\lambda)\equiv(1/N)\sum_i\delta(\lambda-\lambda_i)$, completes the demonstration of our result (A1).

Secondly, we demonstrate the relationship, Eq. (2.3), between the autocorrelation function $P_0(t)$ and the average distance squared traveled by the particle in a time $t$, $\langle X^2(t)\rangle$. Approximating the discrete sites by a continu-

um $X$, one assumes that the probability to be at $X$ at time $t$, given one started at $X=0$ at $t=0$, is given by the following scaling relationship as $t\to\infty$:

$$P(X,t)=C(t)\phi(X/\xi(t)) , \tag{A7}$$

where $\xi^2=\langle X^2(t)\rangle$ is the average distance squared, and $\phi$ is chosen so that $\phi(0)=1$. The autocorrelation function is just $P_0(t)=P(0,t)=C(t)$. Normalization of $P(X,t)$ requires

$$1=\int dX\, P(X,t)=C\int dX\,\phi(X/\xi)=C\xi\int dy\,\phi(y) , \tag{A8}$$

therefore $\xi\propto 1/C$ or

$$\langle X^2(t)\rangle\propto 1/P_0^2(t) . \tag{A9}$$

## APPENDIX B

In this appendix we wish to calculate the lowest order correction in $R$ to the first order perturbation result, Eq. (3.11), for the splitting in eigenvalues as the system size is doubled. That is, if $\lambda_i$ is an eigenvalue of the system of size $2^{n-1}$, we found that $\lambda_i$ remains on eigenvalue of the system size $2^n$, and new eigenvalue appears separated from $\lambda$ by

$$\delta\lambda_i(n)=2\left[\frac{R}{2}\right]^{n-1}[1+bR+O(R^2)] . \tag{B1}$$

Here we wish to calculate the coefficients $b$ of this lowest-order correction and show explicitly that it does not depend on the system size $n$.

To second order in perturbation theory, the correction to the eigenvalue is given by Rayleigh-Schrödinger perturbation theory as

$$\delta\lambda_i^{(2)}(n)=\sum_{j\neq i}\frac{|\langle\psi_i^{(0)}(n)|M_1(n)|\psi_j^{(0)}(n)\rangle|^2}{\lambda_i^{(0)}(n)-\lambda_j^{(0)}(n)} . \tag{B2}$$

We do the calculation for the lowest nonzero eigenvalue $\lambda_1$. Others may be alone similarly. The eigenvalue structure for four levels of matrices of sizes $2^{n-3}$, $2^{n-2}$, $2^{n-1}$, and $2^n$ is shown in Fig. 11. We have labeled the eigenstates of the lowest level according to their symmetry with respect to reflection about the central barrier. Since $M_1$ is symmetric in reflections, only eigenstates of the same symmetry will have a nonzero matrix element. Thus the lowest order in $R$ term in (B2) will come from the state with closest eigenvalue, and the same symmetry. For $\lambda_1$,

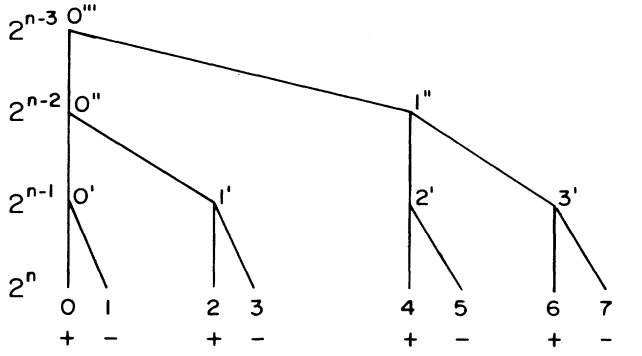


FIG. 11. Low-lying eigenvalue structure for four levels of matrices of sizes $2^{n-3},\ldots,2^n$. The lines indicate how each eigenvalue of a system of size $2^{m-1}$ splits into two new ones in the system of size $2^m$ (see also Fig. 3). The splitting at size $2n$ is $O(R^{n-1}/2^{n-2})$. The zeroth-order perturbation value of an eigenvalue is given by the parent eigenvalue of the system of half the size. The eigenstates at the lowest level $2^n$ have been labeled ($\pm$) to indicate their symmetry with respect to reflection about the central barrier. Only states with equal symmetry are coupled in perturbation.

this correction comes from the coupling between $\psi_1^{(0)}(n)$ and $\psi_3^{(0)}(n)$. We have for the zeroth-order eigenvalues of the states: $\lambda_1^{(0)}(n)=\lambda_0(n-1)=0$; and $\lambda_3^{(0)}(n)=\lambda_1(n-1)=2(R/2)^{n-2}[1+O(R)]$ by the first-order result of Eq. (3.11). The matrix elements of $\psi_1^{(0)}$ and $\psi_3^{(0)}$ are $[1/(2^n)^{1/2}][\pm 1+O(R^{n-1})]$. Combining these results we get to lowest order in $R$,

$$\delta\lambda_1^{(2)}(n)=\frac{|\langle\psi_1^{(0)}(n)|M_1(n)|\psi_3^{(0)}(n)\rangle|^2}{\lambda_1^{(0)}(n)-\lambda_3^{(0)}(n)}=\frac{\left[\frac{4}{2^n}R^{n-1}\right]^2}{2\left[\frac{R}{2}\right]^{n-2}}=-2\left[\frac{R}{2}\right]^n . \tag{B3}$$

Combining with the first order result (3.11) gives

$$\delta\lambda_1(n)=2\left[\frac{R}{2}\right]^{n-1}\left[1-\frac{R}{2}+\cdots\right] , \tag{B4}$$

or $b=\frac{1}{2}$ in Eq. (B1). Note that $b$ does not depend on the matrix size $n$.

[1]R. G. Palmer, D. L. Stein, E. Abrahams, and P. W. Anderson, Phys. Rev. Lett. **53**, 958 (1984).

[2]R. Kohlrausch, Ann. Phys. (Leipzig) **12**, 393 (1847); K. L. Ngai, Comments Solid State Phys. **9**, 127 (1979); **9**, 141 (1980).

[3]J. Tauc, Semicond. Semimetals **21B**, 299 (1984); Z. Vardeny, P. O'Connor, S. Ray, and J. Tauc, Phys. Rev. Lett. **44**, 1267 (1980).

[4]J. Klafter, A. Blumen, and G. Zumofen, Philos. Mag. B **53**, L29 (1986).

[5]V. Dotsenko, J. Phys. C **18**, 6023 (1985); R. V. Chamberlain, G. Mozurkewich, and R. Orabach, Phys. Rev. Lett. **52**, 867 (1984); W. Kinzel, Phys. Rev. B **19**, 4595 (1979).

[6]G. Zumofen, A. Blumen, and J. Klafter, J. Chem. Phys. **84**, 6679 (1986).

[7]A. Ansari, J. Berendzen, S. F. Bowne, H. Frauenfelder, I. E. T.

Iben, T. B. Sauke, E. Shyamsunder, and R. D. Young, Proc. Nat'l. Acad. Sci. U. S. A. **82**, 5000 (1985).
[8]S. B. Oseroff, D. Clarke, S. Schultz, and S. Shtrikman, IEEE Trans. Magn. **MAG-21**, 1495 (1985).
[9]S. Alexander and R. Orbach, J. Phys. (Paris) Lett. **43**, L625 (1982).
[10]J. Klafter and M. F. Schlesinger, Proc. Nat'l. Acad. Sci. U. S. A. **83**, 848 (1986).
[11]A. T. Ogielski and D. L. Stein, Phys. Rev. Lett. **55**, 1634 (1985); M. Schreckenberg, Z. Phys. B **60**, 4831 (1985); S. Grossman, F. Wegner, and K. H. Hoffman, J. Phys. (Paris) Lett. **46**, L575 (1985); G. Paladin, M. Mézard, and C. De Dominicis, J. Phys. (Paris) Lett. **46**, L985 (1985); C. P. Bachas and B. A. Huberman, Phys. Rev. Lett. **57**, 1965 (1986).
[12]B. Huberman and M. Kerszberg, J. Phys. A **18**, L331 (1985).
[13]S. Teitel and E. Domany, Phys. Rev. Lett. **55**, 2176 (1985).
[14]S. Alexander, J. Bernasconi, W. R. Schneider, and R. Orbach, Rev. Mod. Phys. **53**, 175 (1981).
[15]R. Landauer, Helv. Phys. Acta **56**, 847 (1983); M. Buttiker and R. Landauer, in *Nonlinear Phemomena at Phase Transitions and Instabilities,* edited by T. Riste (Plenum, New York, 1982), p. 111.
[16]R. Zwanzig, J. Stat. Phys. **28**, 127 (1982).
[17]E. Domany, S. Alexander, D. Bensimon, and L. P. Kadanoff, Phys. Rev. B **30**, 2752 (1984).
[18]S. Sarker, Phys. Rev. B **30**, 2752 (1984).
[19]H. Vogel, Z. Phys. **22**, 645 (1921); G. S. Fulcher, J. Am. Ceram. Soc. **8**, 339 (1925).
[20]N. G. Van Kampen, *Stochastic Processes in Physics and Chemistry* (North-Holland, Amsterdam, 1981), Chaps. 5 and 6.
[21]The discussion so far is consistent also with a marginally unstable fixed point at $R=0$. The existence of a line of fixed points is shown below.
[22]A. Maritan and A. L. Stella, J. Phys. A **19**, L269 (1986) and Phys. Rev. Lett. **56**, 1754 (1986).
[23]S. Teitel and E. Domany, Phys. Rev. Lett. **56**, 1755 (1986).
[24]We have no rigorous proof of this result, however calculation of a few terms explicitly should convince the reader of its validity. As an example we calculate the first-order correction to $\lambda_1$ in Appendix B.
[25]P. Dean, Rev. Mod. Phys. **44**, 127 (1972).
[26]Y. Imry, J. Appl. Phys. **52**, 1817 (1981).
[27]One takes a finite segment of length $N$, repeated periodically many times. See Ref. 16 and also B. Derrida, J. Stat. Phys. **31**, 433 (1983).
[28]C. Henley, Phys. Rev. Lett. **54**, 2030 (1985).
[29]For a one-dimensional hierarchically coupled Ising spin model see D. Kutasov, A. Aharony, E. Domany, and W. Kinzel, Phys. Rev. Lett. **56**, 2229 (1986).
[30]For a review, see G. S. Grest and M. H. Cohen, in *Advance in Chemical Physics,* edited by I. Prigogine and S. Rice (Wiley, New York, 1981), Vol. 48.
[31]S. P. Das, G. F. Mazenko, S. Ramaswamy, and J. Toner, Phys. Rev. Lett. **54**, 118 (1985).
[32]J. J. Ullo and S. Yip, Phys. Rev. Lett. **54**, 1509 (1985).